ECS Transactions, 61 (4) 329-336 (2014)
10.1149/06104.0329ecst ©The Electrochemical Society

# Ti/Al/Ni/Cu Ohmic Contact with Low Contact Resistance and Smooth Surface Morphology for AlGaN/GaN HEMT

Y.-Y. Wong [a], E. Y. Chang [a], Y.-K. Chen [b], S.-C. Liu [a], Y.-C. Lin [a], J.-S. Maa [b]

[a] Department of Materials Science and Engineering, National Chiao Tung University, Hsinchu 30010, Taiwan.
[b] Institute of Lighting and Energy Photonics, National Chiao Tung University, Tainan 71150, Taiwan

The feasibility of replacing the Au layer in a conventional ohmic contact of Ti/Al/Ni/Au for AlGaN/GaN structure with Cu has been investigated. While the thicknesses of Ti, Al and Cu layers were fixed throughout the study, the thickness of Ni layer was varied to examine its influence on the Cu-based ohmic contacts. It is showed that the Ni layer thickness played an important role in the Ti/Al/Ni/Cu metallization for achieving low contact resistance and smooth surface morphology. With a 50-Å Ni layer, a low specific contact resistance ($r_c$) of $1.35\times10^{-6}$ ohm-cm$^2$ has been realized. This result is comparable with the conventional ohmic contact ($r_c = 1.19\times10^{-6}$ ohm-cm$^2$). High electron mobility transistor (HEMT) devices fabricated using both Au- and Cu-based ohmic contact exhibited similar DC characteristics, suggesting that the electrical performance did not degrade with the used of Cu in the ohmic contact. Furthermore, in the absence of Au, the surface roughening caused by Au-Al alloy in the conventional ohmic contact was also prevented. As a result, the root-mean-square roughness of the optimized Cu-based contact was only 7.62 nm as compared to 134 nm for the conventional structure.

## Introduction

Dramatic development in GaN semiconductor materials in the last decade has led to the rapid development of high performance electronic devices especially high electron mobility transistors (HEMTs). The most favorable heterostructure for GaN HEMT is AlGaN/GaN. Due to its high energy bandgap and high electron saturated velocity, AlGaN/GaN HEMT becomes an ideal candidate for device operating at high frequency, high output current and high breakdown voltage applications [1, 2]. In order to realize the potential of the GaN devices, a good ohmic contact metallization with both low contact resistance and smooth surface morphology is required. The most widely used ohmic metal for AlGaN/GaN HEMT devices consist of a Ti/Al bilayer. Upon high temperature annealing (750~950 °C), Ti and Al will react with GaN to form low resistance ohmic contact [3, 4]. On top of the Ti/Al bilayer, an oxidation preventive layer, also with low resistance, such as Au will be deposited as the contact pads. In order to prevent the diffusion of Au into the semiconductor, a diffusion barrier layer (such as Ni, Pt, Cr or Mo) will be inserted in between the Ti/Al and Au layers. By optimizing the thickness of each metal layer and its annealing condition, low specific contact resistance ($r_c$) of $4.7 \times 10^{-7}$ Ω-cm [5] and $7.3 \times 10^{-7}$ Ω-cm [6] have been realized for ohmic structure of Ti/Al/Mo/Au and Ti/Al/Ni/Au, respectively.

Gold has been widely used in the semiconductor industry for many years due to its low resistivity and high resistance to oxidation. However, the high and ever rising of gold price has


Downloaded on 2014-12-24 to IP 140.113.38.11 address. Redistribution subject to ECS terms of use (see ecsdl.org/site/terms_use) unless CC License in place (see abstract).

led to the aggressive searching of an alternative material, such as copper (Cu), to replace the Au as metallization material in the Si VLSI technology [7, 8]. As compared to Au, Cu has several advantages including lower resistivity (1.67 μΩ-cm for Cu; 2.2 μΩ-cm for Au) [9, 10], better thermal conductivity (4.01 $Wcm^{-1}K^{-1}$ for Cu; 3.18 $Wcm^{-1}K^{-1}$for Au) and much lower cost (Cu is 400 times cheaper than Au). Furthermore, Cu has also been demonstrated to perform well as the gate [11, 12] and as the interconnect [13] materials on the GaN HEMT devices. Nonetheless, the main problem of using Cu on semiconductor devices is its high diffusivity [14]. The diffusion of Cu into semiconductor material especially GaN is shown to be detrimental to its devices performances [15-17]. This hinders the usage of Cu as the ohmic contact material for GaN HEMT because high annealing temperature is always required for good ohmic contact formation. Researchers were looking into ways of making ohmic contact with lower annealing temperatures. Ohmic structures such as Si/Ti/Al/Cu/Au [18], Ge/Cu/Ge [19] and Ti/Cu/Ge [20] have been successfully formed at lower temperature (< 800 °C). However, these structure were all having relatively high contact resistance ($r_c > 10^{-5}$ Ω-cm) and thus limited their usefulness. In this study, the structure of Ti/A/Ni/Cu was proposed as ohmic contact material for AlGaN/GaN HEMT devices. We replaced the top layer of Au in an conventional Ti/Al/Ni/Au ohmic contact with Cu but maintaining the Ti/Au bilayer since it is proven advantageous for low resistance ohmic contact formation. Besides, the role of Ni as a diffusion barrier and the formation mechanism of Ti/Al/Ni/Cu ohmic contact will also be investigated.

## Experimental

The Ti/Al/Ni/Cu ohmic contact was formed on the GaN HEMT structure grown on 6-inch Si (111) substrate. The structure of the epitaxial layer is illustrated in Figure 1. Before ohmic metal deposition, the wafers were first rinsed in acetone and isopropanol to remove organic contaminants and then followed by buffer hydrofluoric acid solution to etch away the native oxide. Standard optical I-line exposure process was used to define the pattern for ohmic metal deposition. Four samples with different Ni layer thicknesses, as shown in Table I were prepared to investigate the role of Ni played in Ti/Al/Ni/Cu ohmic structure. The thicknesses of Ti and Al layers for these samples were fixed at 200 Å, and 1200 Å, respectively. Furthermore, both the Cu and Au layer thicknesses were also kept the same at 1000 Å. In fact, the sample D used a standard ohmic metal scheme with gold metallization and thus acted as a control sample. All the ohmic metals were deposited using an E-beam evaporator except the copper layer which was deposited using a sputtering machine. Annealing process was performed in a rapid thermal annealing (RTA) system at 900 °C for 30 s under pressure of $5\times10^{-6}$ torr in $N_2$ ambient. Finally, mesa isolation was achieved with $Cl_2$/Ar inductively coupled plasma etching to a depth of approximately 200 nm, which is well below the 2-dimensional electron gas (2DEG) channel. Two set of samples were prepared: one for electrical properties measurement and the other for material characterization. The specific contact resistances of these samples were measured with an Agilent E5270 system using transmission line model (TLM) method. The contact pads on the TLM pattern were separated by various spacing (3, 5, 10, 20 and 36 μm). HEMT device were also fabricated on selected samples to check their DC performances. The HEMT devices fabricated in this study had a 7-μm source-drain spacing and a 2-μm gate length. The gate contacts were formed by $W_xN$ (200Å)/Cu (1000Å) metal deposition using a sputtering system. The $W_xN$ is a stable material for gate contact as studied in a previous work [21]. An optical microscope (OM) and an atomic force microscope (AFM, Digital Instrument,


Downloaded on 2014-12-24 to IP 140.113.38.11 address. Redistribution subject to ECS terms of use (see ecsdl.org/site/terms_use) unless CC License in place (see abstract).

D3100) were used to examine the surface morphology of the ohmic structure after high temperature annealing. Besides, depth profiling Auger electron spectroscopy (AES, Microlab 350) was performed to investigate the intermixing of metal layers. Grazing incident angle X-ray diffraction (XRD, Bede D1) and cross-sectional transmission electron microscopy (TEM, JEOL 2100F) were also employed to investigate the formation of various metallic compounds and their microstructures, respectively, in the ohmic metal. The chemical elements presented in the metallic microstructure were determined by an energy-dispersive X-ray spectroscopy (EDS, Link ISIS 300) attached to the TEM system.

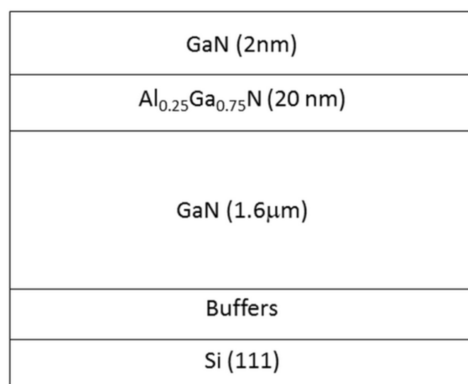


Figure 1. Schematic diagram of AlGaN/GaN HEMT structure on Si substrate.

**TABLE I**. Ohmic contact structures with different Ni layer thicknesses.

| Sample | Ohmic Structure | Ni Thickness |
|---|---|---|
| A | Ti/Al/Cu | 0 |
| B | Ti/Al/Ni/Cu | 50 Å |
| C | Ti/Al/Ni/Cu | 250 A |
| D | Ti/Al/Ni/Au | 250 Å |

## Results and discussion

Figure 2 summarized the $r_c$ values of sample A to D. The result shows that the Ni layer thickness played an important role for the ohmic contact structure of Ti/Al/Ni/Cu. Sample B with a 50-Å Ni has the lowest $r_c$ among the Cu-based ohmic contact samples with a value of $1.35\times10^{-6}$ Ω-cm$^2$. This value is comparable with that of a conventional ohmic contact scheme (sample D, with an $r_c$ of $1.19\times10^{-6}$ Ω-cm$^2$). On the other hand, the $r_c$ increased by almost 1 and 2 orders of magnitudes higher for sample without the Ni layer (sample A) and for sample with a 250-Å thick Ni layer (sample C), respectively. Furthermore, the sample A also has the worst surface morphology, as shown in figure 3 (a), with serious metal peeling problem. Due to this problem, the sample A was omitted for further investigation. The thin Ni layer is seemed to be able to avoid the formation of intermetallic compound and cavities following a direct contact of Cu and Al [22]. The peeling problem reduced the contact area between the ohmic metal and semiconductor and thus increased the contact resistance. For sample with thicker Ni layer (sample C), the increased of $r_c$ may be due to the increased of metal resistance for a thicker


Downloaded on 2014-12-24 to IP 140.113.38.11 address. Redistribution subject to ECS terms of use (see ecsdl.org/site/terms_use) unless CC License in place (see abstract).

metal layer. This result is also observed in the conventional Ti/Al/Ni/Au structure [6].

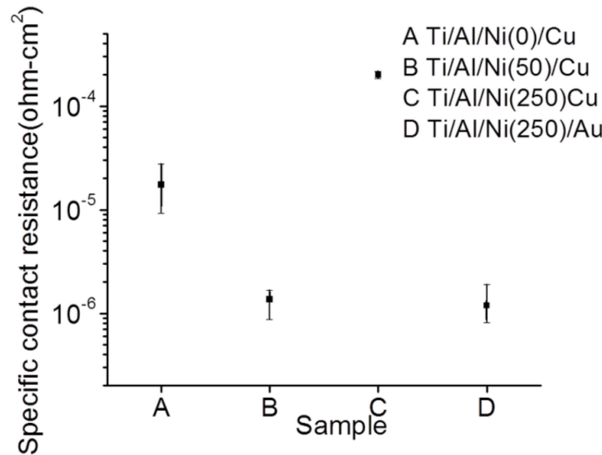


Figure 2. Specific contact resistance of different ohmic metal structures. The numbers in the legend are the Ni layer thickness in angstrom.

Besides contact resistance, the surface morphology of the ohmic contact is also investigated. It is known that the Ti/Al/Ni/Au ohmic contact has a very rough surface, which may be induced by the formation of Au-Al and NiAl alloys [23]. As shown in Figure 3 (c) and 3 (f), the Ti/Al/Ni/Au has a root-mean-square (rms) roughness of 134 nm. The rough surface of ohmic contact may cause poor edge acuity, which is undesirable for short-channel device fabrication. In contrast, the surfaces of the Ti/Al/Ni/Cu structures were relatively smooth (Figure 3 (b), 3 (d) and 3 (e)). Sample B, with 50-Å Ni, not only has the lowest contact resistance but also the smoothest surface morphology (rms = 7.62 nm). The surface roughness of sample C, with a much thicker Ni layer (250 Å), increased slightly to 12.50nm. This result suggested that the Au-Al, rather than the NiAl, played a much more significant role in the roughening of Ti/Al/Ni/Au ohmic contact.

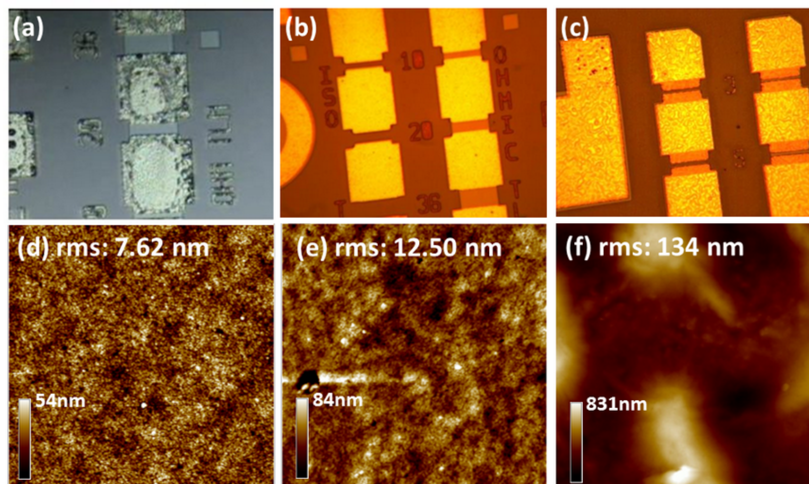


Figure 3. Optical microscopy images of (a) Ti/Al/Cu, (b) Ti/Al/Ni (50Å)/Cu, and (c) Ti/Al/Ni(250Å)/Au. AFM images of 10 μm x 10 μm area for ohmic contact with (d) Ti/Al/Ni (50Å)/Cu, (e) Ti/Al/Ni(250Å)/Cu and (f) Ti/Al/Ni(250Å)/Au structure.


Downloaded on 2014-12-24 to IP 140.113.38.11 address. Redistribution subject to ECS terms of use (see ecsdl.org/site/terms_use) unless CC License in place (see abstract).

Figure 4 shows the depth profiling AES analyses of the sample B (Ti/Al/Ni(50-Å)/Cu) before and after annealing. Before annealing, all the deposited metal layers had a clear boundary with minimum inter-diffusion. The small Ni spectrum that seemed embedded in that of Cu and Al is because it was very thin (5 nm) and its boundaries could not be resolved by the AES. On the other hand, intermixing of various metal layers was clearly observed for sample after annealing (Figure 4 (b)). Even though the Cu diffused towards the semiconductor but was seen stopped at a depth corresponding to the initial Ti thickness. All other elements including Ga, which originated from the semiconductor layers, out-diffused towards the surface. The thin Ni did not seem to be an effective diffusion barrier for Cu. It is believed that the formation of various compounds in the metal stack had prevented the in-diffused of Cu. XRD and TEM analyses shown in Figure 5 would support this hypothesis.

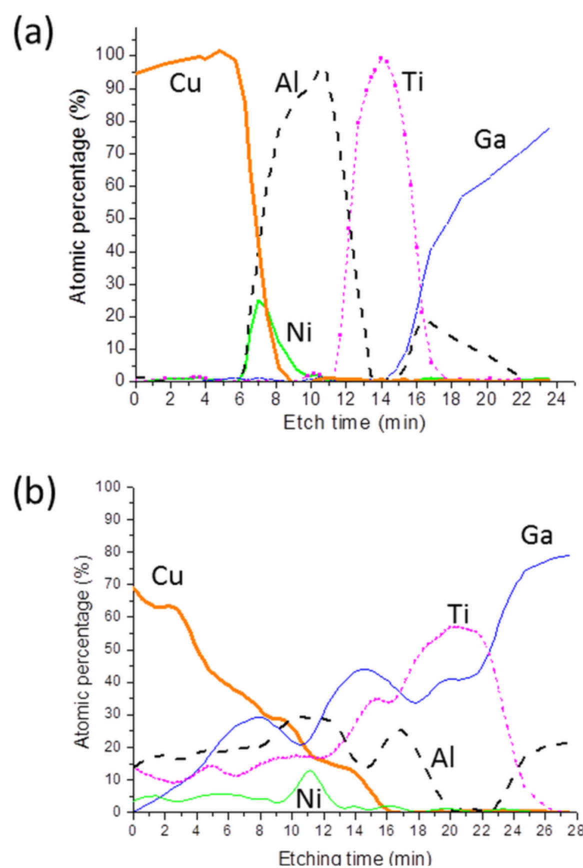


Figure 4. Depth profiling Auger results of Ti/Al/Ni (50Å)/Cu ohmic contact (a) before and (b) after annealing.

The XRD result shown in Figure 5 (a) reveals that various alloys, especially Al-Cu and Ti-Cu based alloys were formed upon high temperature annealing. A strong XRD peak appeared at around 44.25°could probably be attributed to the $Al_4Cu_9$ (2θ = 44.22°), AlNi (2θ = 44.31°), and $CuGa_2$ (2θ = 44.39°) (inset of Figure 5 (a)). The $CuGa_2$ was associated with the out-diffusion of Ga as shown in the AES spectrum. Other Cu-based compounds found included CuTi (2θ = 41.11°) and $Cu_4Ti_3$ (2θ = 75.64°). Besides this, compounds that normally occurred


Downloaded on 2014-12-24 to IP 140.113.38.11 address. Redistribution subject to ECS terms of use (see ecsdl.org/site/terms_use) unless CC License in place (see abstract).

in a Ti/Al-based ohmic contact such as AlTi (2θ = 38.72°) and TiN (2θ = 36.62°) [24] were also observed. In additional to the XRD result, the cross-sectional TEM image shown in Figure 5 (b) reveals the distribution of various compounds in the Ti/Al/Ni/Cu ohmic contact. Generally, the chemical compositions of these compounds, as determined by EDS, were in good agreement with the XRD result. The $Al_xCu_y$ alloys dominated the Cu-based ohmic metal compounds. Besides, the out-diffusion of Ti and Al atoms had led to the formation of CuTi (at the surface) and AlNi (near the initial location of Ni layer). Similar to the case of Ti/Al/Ni/Au ohmic contact, a thin polycrystalline TiN layer was also clearly observed at the Ti-GaN interface when Ti was first deposited on the GaN materials [4 24, 25]. This layer played an important role in achieving low contact resistance for the Ti/Al-based ohmic contact because the formation of TiN could lead to the supersaturation of nitrogen vacancies at the semiconductor surface to generate a highly N-doped layer [26, 27]. The EDS performed on the AlGaN layer near to the metal/semiconductor interface also shows that no Cu diffused into the semiconductor layer (inset of Figure 5 (b)). Both XRD and TEM results suggested that no evident of Cu diffusion into the semiconductor layers. Furthermore, no pure metallic XRD peak or TEM microstructure were detected. This implied that all the deposited pure metals, including Cu, had been transformed into various alloys especially the Al-Cu and Ti-Cu based alloys. These alloys were thermally more stable than the pure Cu and thus formed stable ohmic contact for GaN devises.

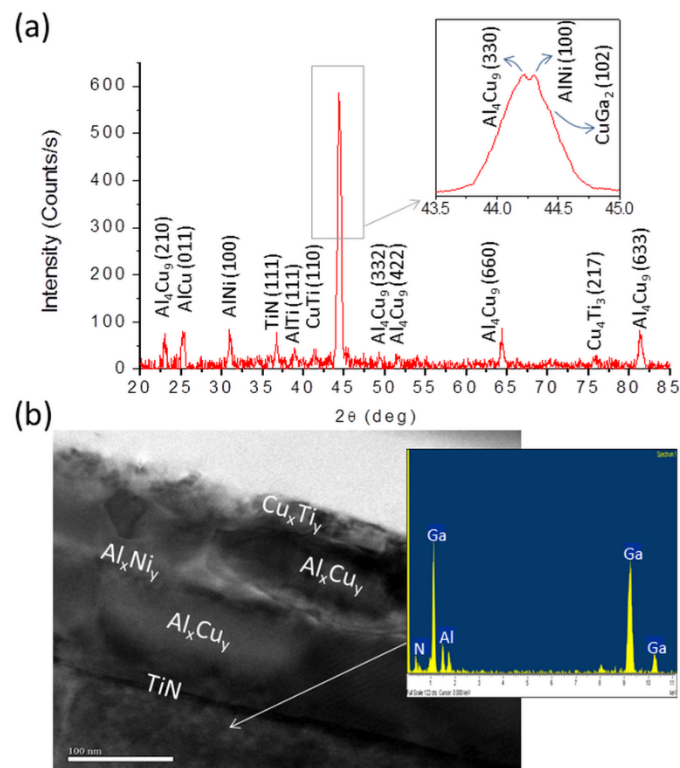


Figure 5 (a) XRD result and (b) TEM image of Ti/Al/Ni(50Å)/Cu ohmic contact structure.

Finally, AlGaN/GaN HEMT devices were also fabricated using the ohmic contact of Ti/Al/Ni(50-Å)/Cu and the gate contact of $W_xN$/Cu. The DC characteristic of the HEMT device


Downloaded on 2014-12-24 to IP 140.113.38.11 address. Redistribution subject to ECS terms of use (see ecsdl.org/site/terms_use) unless CC License in place (see abstract).

is shown in Figure 6. It has a maximum drain current ($I_{Dmax}$) of 370 mA/mm, a transconductance (Gm) of 128 mS/mm and an off-state breakdown voltage ($V_{BK}$) of 136 V. This result is comparable with HEMT device fabricated using the conventional ohmic contact of Ti/Al/Ni/Au (not shown here). Besides the material analyses, the good ohmic contact and DC performances of the HEMT device also supported the idea that the Cu had been completed consumed and no trace was left to contact with or diffuse into the semiconductor. The current study suggested that the Cu can be used to replace the Au layer as ohmic contact material for AlGaN/GaN structure if the device reliability issue can be addressed in the future.

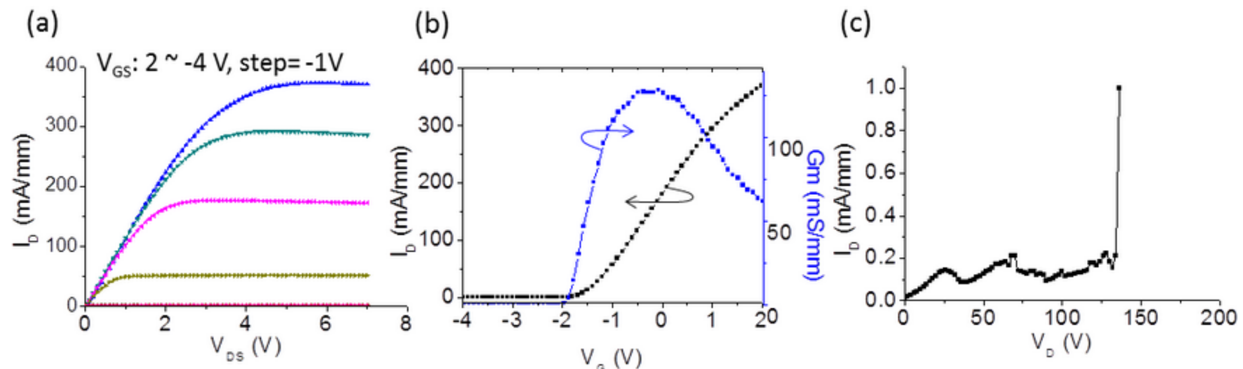


Figure 6 DC performance of HEMT device fabricated using Ti/Al/Ni (50Å)/Cu ohmic contact; (a) $I_D$-$V_{DS}$ curves, (b) Gm and $I_D$ versus $V_G$ curves, and (c) off-state breakdown characteristic.

## Conclusion

The feasibility of using Ti/Al/Ni/Cu as ohmic contact for AlGaN/GaN HEMT device has been investigated. The Ni layer played an important role to avoid the direct contact of Cu with the Al layer. By optimizing the Ni layer thickness (50 Å), ohmic contact with low specific contact resistance of $1.35\times10^{-6}$ ohm-cm$^2$ and smooth surface morphology of 7.62 nm had been achieved. The low contact resistance could be attributed to the formation of TiN alloy as for the case of Ti/Al/Ni/Au structure. Furthermore, in the absence of Au, the formation of Au-Al alloys, which caused the roughening of Ti/Al/Ni/Au ohmic contact, was also prevented. Both material and electrical analyses suggested that no Cu diffused into the semiconductor layer. All the Cu had been consumed to form a more stable Al-Cu and Ti-Cu based alloys. This study implies that the Ti/Al/Ni/Cu structure has a great potential to be used as ohmic contact for AlGaN/GaN HEMT devices.

## Acknowledgements

This work was sponsored in part by the Ministry of Economy Affairs and in part by the NCTU-UCB I-RiCE program of National Science Council, Taiwan, under Grant Nos. 101-EC-17-A-05-S1-154 and NSC103-2911-I-009-302.

## References


1. N. Onojima, N. Hirose, T. Mimura, and T. Matsui, Jpn. J. Appl. Phys. **48**, 094502 (2009).
2. A. Chini, R. Coffie, G. Meneghesso, E. Zanoni, D. Buttari, S. Heikman, S. Keller, and U.




Downloaded on 2014-12-24 to IP 140.113.38.11 address. Redistribution subject to ECS terms of use (see ecsdl.org/site/terms_use) unless CC License in place (see abstract).

K. Mishra, Electron. Lett. **39**, 625 (2003).
[3] B. P. Luther, S. E. Mohney, T. N. Jackson, M. A. Khan, Q. Chen, and J. W. Yang, Appl. Phys. Lett. **70**, 57 (1997).
[4] S. Ruvimov, Z. Liliental-Weber, J. Washburn, K. J. Duxstad, E. E. Haller, Z.-F. Fan, S. N. Mohammad, W. Kim, A. E. Botchkarev, and H. Morkoc, Appl. Phys. Lett. **69**, 1556 (1996).
[5] V. Kumar, L. Zhou, D. Selvanathan, and I. Adesida, J. Appl. Phys. **92**, 1712 (2002).
[6] B. Jacobs, M. C. J. C. M. Kramer, E. J. Geluk, and F. Karouta, J. Cryst. Growth **241**, 15 (2002).
[7] M. Moriyama, T. Kawazoe, M. Tanaka, and M. Murakami, Thin Solid Films **416**, 136 (2002).
[8] V. S. C. Len, R. E. Hurley, N. McCusker, D. W. McNeill, B. M. Armstrong, and H. S. Gamble, Solid-State Electron. **43**, 1045 (1999).
[9] J. R. Lloyd, J. Clemens, and R. Snede, Microelectron. Reliab. **39**, 1595 (1999).
[10] J. D. Plummer, M. Deal, and P. D. Griffin, *Silicon VLSI Technology: Fundamentals, Practice, and Modeling* (Prentice Hall, Upper Saddle River, NJ, 2000).
[11] J.-P. Ao, D. Kikuta, N. Kubota, Y. Naoi, and Y. Ohno, IEEE Electron Device Lett. **24**, 500 (2003).
[12] H. F. Sun, A. R. Alt, and C. R. Bolognesi, IEEE Electron Device Lett. **28**, 350 (2007).
[13] Y.-C. Lin, T.-Y. Kuo, Y.-L. Chuang, C.-H. Wu, C.-H. Chang, K.-N. Huang, and E. Y. Chang, Appl. Phys. Express **5**, 066503 (2012).
[14] A. A. Istratov and E. R. Weber, J. Electrochem. Soc. **149**, G21 (2002).
[15] J.-P. Ao, N. Kubota, D. Kikuta, Y. Naoi, and Y. Ohno, Phys. Status Solidi C **0**, 2376 (2003).
[16] J. Park, K. Lee, H. Y. Cha, and K. Seo, Electron. Lett. **46**, 1011 (2010).
[17] V. Rajagopal Reddy and P. Koteswara Rao, Microelectron. Eng. **85**, 470 (2008).
[18] C. J. Youn and M. S. Han, J. Korean Phys. Soc. **39**, 723 (2001).
[19] M. Schuette and W. Lu, J. Electron. Mater. **36**, 420 (2007).
[20] N. Mahadik, M. Rao, and A. Davydov, J. Electron. Mater. **35**, 2035 (2006).
[21] C. Y. Lu, E. Y. Chang, J. C. Huang, C. T. Chang, and C. T. Lee, Electron. Lett. **45**, 1348 (2009).
[22] C. J. Hang, C. Q. Wang, M. Mayer, Y. H. Tian, Y. Zhou, and H. H. Wang, Microelectron. Reliab. **48**, 416 (2008).
[23] R. Gong, J. Wang, S. Liu, Z. Dong, M. Yu, C. P. Wen, Y. Cai, and B. Zhang, Appl. Phys. Lett. **97**, 062115 (2010).
[24] K. H. Kim, C. M. Jeon, S. H. Oh, J.-L. Lee, C. G. Park, J.-H. Lee, K. S. Lee, and Y.-M. Koo, J. Vac. Sci. Technol. B: Microelectronics and Nanometer Structures **23**, 322 (2005).
[25] A. Motayed, A. V. Davydov, W. J. Boettinger, D. Josell, A. J. Shapiro, I. Levin, T. Zheleva, and G. L. Harris, Phys. Status Solidi C **2**, 2536 (2005).
[26] D. W. Jenkins, J. D. Dow, and M.-H. Tsai, J. Appl. Phys. **72**, 4130 (1992).
[27] F. Iucolano, F. Roccaforte, A. Alberti, C. Bongiorno, S. D. Franco, and V. Raineri, J. Appl. Phys. **100**, 123706 (2006).


Downloaded on 2014-12-24 to IP 140.113.38.11 address. Redistribution subject to ECS terms of use (see ecsdl.org/site/terms_use) unless CC License in place (see abstract).